Levels of ^{88}Sr from the ^{86}Sr$(t,p)^{88}$Sr Reaction*

R. C. Ragaini,† J. D. Knight, and W. T. Leland
University of California, Los Alamos Scientific Laboratory, Los Alamos, New Mexico 87544
(Received 22 April 1970)

The levels of ^{88}Sr up to an excitation energy of 7 MeV have been investigated by the ^{86}Sr(t,p) reaction with 15-MeV tritons. Proton spectra were measured by a ΔE-E counter telescope system with an over-all resolution of 35 keV, and close-lying peaks were resolved by additional measurements with a magnetic spectrograph. Angular distributions were measured from 12.5 to 90°, and comparisons with zero-range distorted-wave Born-approximation calculations permitted spin assignments of 32 of the 45 levels observed. Four excited 0^+ states were observed. From a comparison of their cross sections with the ^{88}Sr$(t,p)^{90}$Sr ground-state cross section, no one of them could be identified as the pairing vibration state; the strength of the latter appears to be fragmented. The data are compared with previous information on the ^{88}Sr level structure.

I. INTRODUCTION

Of the $N=50$ nuclei, ^{88}Sr and ^{90}Zr offer probably the best starting point for analysis of proton and neutron interactions. The energy gap between the filled-neutron-shell configuration $(2p_{1/2})^2(1g_{9/2})^{10}$ and the first shell-crossing configurations $(2p_{1/2}$ or $1g_{9/2})^{-1}(2d_{5/2})^1$ is of the order of 4 MeV, and thus the levels below this energy must be contributed principally by proton excitations. For ^{88}Sr, with $Z=38$, the dominant ground-state proton configuration is the closed subshell $(1f_{5/2})^6(2p_{3/2})^4$, and the first few excited states are expected to involve population of the $(2p_{1/2})$ and $(1g_{9/2})$ orbitals with corresponding holes in the $(1f_{5/2})$ and $(2p_{3/2})$ orbitals.

Recent years have seen a considerable interest in the ^{88}Sr level structure. The first theoretical approaches for the $N=50$ nuclei involved only the proton excitations, and the calculations employed the effective-interaction method[1,2] and proton one-particle–one-hole (1p-1h) finite-range forces.[3] More-recent calculations have taken into account neutron 1p-1h configurations as well, and reasonable results have been obtained for ^{88}Sr.[4,5] Neutron 1p-1h excitations of the $N=50$ core have been included also in calculations based on Tamm-Dancoff and random-phase approximations.[6,7]

Experimental data on ^{88}Sr have been obtained in a number of measurements. Collective properties of several of the levels have been investigated by inelastic scattering of protons,[8,9] deuterons,[10] α particles,[11] and electrons.[12] Proton 1p-1h states incorporating a $(2p_{1/2})$ particle have been observed in the ^{89}Y$(d,{}^3$He$)^{88}$Sr reaction[13] and the ^{89}Y$(t,\alpha)^{88}$Sr reaction[14]; these results have shown, as expected, that the lowest-lying excited states of ^{88}Sr derive mainly from proton excitations. Neutron 1p-1h states based on a $(1g_{9/2})$ hole have been studied by the ^{87}Sr$(d,p)^{88}$Sr reaction,[15] and the results have demonstrated that these neutron configurations appear only at excitations above 4 MeV, except for small fragments admixed into the lower-lying states. Some preliminary data on the ^{86}Sr$(t,p)^{88}$Sr reaction have been reported by Glover and McGregor.[16] Additional information on the level structure of ^{88}Sr has been obtained from studies of the radioactive decay of ^{88}Rb[17-21] and ^{88}Y[22] and of γ rays from ^{87}Sr neutron capture.[23-26]

The present work employs the two-neutron stripping reaction to study the neutron 2p-2h and 1p-1h components of the ^{88}Sr levels. Since the neutron configuration of the ^{86}Sr target nucleus is largely a mixture of the components $(1g_{9/2})^{-2}$, $(2p_{1/2})^{-2}$, and $(2p_{3/2})^{-2}$, the (t,p) reaction populates those ^{88}Sr states which have neutron components of the 2p-2h type $(1g_{9/2})^{-2}(2d_{5/2})^2$, etc., most of which cannot be populated by any other reaction, as well as of the 1p-1h type $(2p_{1/2})^{-1}(2d_{5/2})^1$, etc.

II. EXPERIMENTAL PROCEDURE

The experiments were carried out using 15-MeV incident tritons accelerated at the Los Alamos Tandem Van de Graaff facility. Triton beam currents were typically 300 to 600 nA on target, with the beam spot approximately 1 mm^2. Most of the particle spectra were measured with a semiconductor ΔE-E counter telescope in conjunction with a particle identification system. In addition, four high-resolution measurements were conducted with an Elbek-design broad-range magnetic spectrograph.[27]

A. Targets

For the experiments performed with the counter telescope arrangement, the targets consisted of approximately 75 μg/cm^2 of metallic strontium evaporated onto 50 μg/cm^2 carbon foil from $Sr(NO_3)_2$.

The strontium had the following isotopic composition: ^{86}Sr (97.6%), ^{88}Sr (1.73%), ^{87}Sr (0.68%), ^{84}Sr (<0.05%). Careful examination of the reaction spectra showed no evidence of reactions on strontium isotopes other than ^{86}Sr. For the experiments performed with the magnetic spectrograph, the targets consisted of approximately 100 μg/cm^2 of strontium deposited (probably as nitrate) on 50-μg/cm^2 carbon foil. Deposition was accomplished by the "molecular-plating" technique, in which $Sr(NO_3)_2$ is dissolved in water and mixed with isopropanol, and the solution is introduced into an electrolytic cell of which the carbon foil is the cathode. Targets produced in this manner could withstand up to 1 μA of incident triton beam current, almost twice the current the evaporated targets could tolerate.

B. Counter Telescope and Spectrograph Systems

The semiconductor measurements employed a 20-in.-diam scattering chamber with the ΔE-E counter telescope mounted on a remotely controllable arm. The 3-mm Si(Li) E detector and the 400-μ totally depleted Si surface-barrier ΔE detector were enclosed in a common mount cooled to −20°C by contact with a thermoelectric cooling unit. The accuracy of the angular setting of the telescope arm was ±0.05°, and the angular acceptance of the telescope system, as defined by the entrance slit, was ~0.25°. A 700-μ Si surface-barrier detector mounted at 30° served as a monitor to indicate any changes in the target during bombardments. The ΔE detector thickness was chosen to stop all He particles. Since the range of the highest-energy protons emerging from the ΔE detector exceeded 3 mm of Si, the E detector was turned at 45° to the direction of the incoming particles, thus making it possible to take advantage of the better energy resolution obtainable with the 3-mm detector relative to that with thicker units.

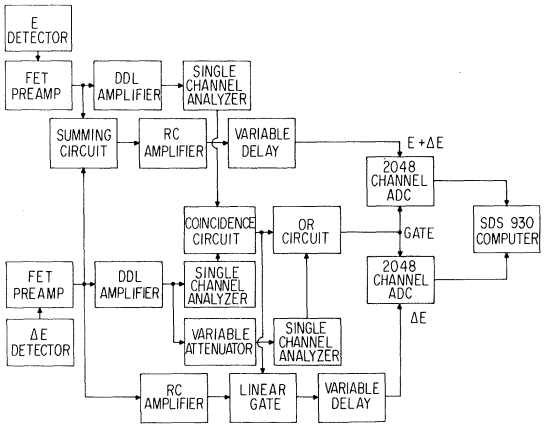

FIG. 1. Schematic diagram of the particle-detection and identification circuitry.

Figure 1 shows a schematic diagram of the particle detection and identification circuitry. When a gate pulse arrived at the analog-to-digital converters (ADC's), the SDS 930 computer read the $(\Delta E + E)$ and ΔE digital pulses from the ADC's. The computer then subtracted ΔE from $(\Delta E + E)$ and generated a mass-charge spectrum (Fig. 2) by calculating Goulding's range-energy approximation[28] in the form

$$m^{0.73}Z^2 = \text{const} \times [(\Delta E + E)^{1.73} - E^{1.73}] .$$

The particle-identification program permitted sorting of the $(\Delta E + E)$ pulses into four adjustable mass-charge bins, in this case protons, deuterons, tritons, and α particles. Once the limits were set on the bins, as shown in Fig. 2, the program was switched to the energy mode and the four spectra could be accumulated. Each particle spectrum consisted of 800 channels, which could be selected as a band from the 2048 channels of the $(\Delta E + E)$ ADC. Since the α particles were all stopped in the ΔE detector, the logic circuitry was set up to store all α particle pulses in the zero channel of the mass-charge spectrum. Details of the data processing system have been reported elsewhere.[29]

Examination of the proton spectra as measured by this system showed that the energy resolution obtained, about 35–40 keV full width at half maximum (FWHM), was insufficient to resolve a number of close-lying peaks, particularly in the regions corresponding to ^{88}Sr excitations near 4 MeV. To obtain better energy and intensity values, and to reveal possible weak peaks which would tend to be concealed in the wings of some of the stronger ones, a series of four proton spectra were measured also on the magnetic spectrograph. Particles were recorded on Eastman 50-μ NTB nuclear-emulsion plates, and over-all resolution was 25 keV FWHM.

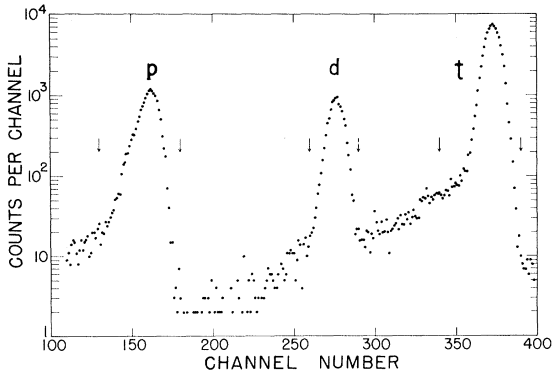

FIG. 2. Mass spectrum generated by mass-identification circuitry. Arrows indicate gated regions for proton, deuteron, and triton groups. Helium-ion pulses were stored in channel zero.

C. Excitation Energies and Cross Sections

Excitation energies of the ^{88}Sr levels were determined by utilizing well-established Q values, together with precisely determined level energies from Ge(Li) γ-ray measurements. The two ends of the excitation energy scale were established from the following Q values calculated from the tables of Mattauch, Thiele, and Wapstra[30]: ^{12}C-$(t,p)^{14}$C, 4.6411±0.0004 MeV; ^{16}O$(t,p)^{18}$O, 3.7068 ±0.0004 MeV; and ^{86}Sr$(t,p)^{88}$Sr, 11.055±0.007 MeV. Errors arising from system nonlinearities were reduced by use of the reported energies[31] of the first two excited states of ^{88}Sr: 1.8361±0.0001 and 2.7341±0.0001 MeV. All of the energies obtained in this study were taken from the spectrograph experiments and were consistent with the counter-telescope data. The listed uncertainties in the energies (Table II) represent only the precision of the spectrograph measurements.

The target thicknesses used in the calculation of the absolute (t,p) cross sections were derived from the analysis of the elastic scattering measurements, as described below. The cross sections as obtained from the spectrograph data were relative; they were converted to absolute values by reference to the 5.165-MeV peak, for which good absolute cross sections had been determined from the counter-telescope experiments. In general, spectrograph intensity data were plotted only where no counter-telescope data existed.

III. EXPERIMENTAL RESULTS

A. Triton Elastic Scattering

The triton elastic scattering angular distributions were measured at 2.5° intervals from 10 to 100°, and were analyzed using an optical-model potential of the Woods-Saxon type:

$$U(r) = V_C - V(e^x + 1)^{-1} - iW(e^{x'} + 1)^{-1},$$

where

$$x = (r - r_0 A^{1/3})/a$$

and

$$x' = (r - r_0' A^{1/3})/a'$$

with the Coulomb potential (V_C) of a uniformly charged sphere of radius $r_0^C A^{1/3}$. The term V represents the real well depth, W the volume absorption term, r_0 and r_0' the radius parameters, and a and a' the diffuseness parameters.

Optimum values of the optical-model parameters were obtained by using Perey's automatic search routine,[32] which searches on those parameters which are preassigned as variables until χ^2 reaches a minimum value, where

$$\chi^2 = N^{-1} \sum_{i=1}^{N} [\sigma_{Th}(\theta_i) - R\sigma_{Ex}(\theta_i)]^2 / \Delta\sigma_{Ex}^2(\theta_i).$$

The measured and predicted cross sections are denoted by σ_{Ex} and σ_{Th}, respectively, where $\Delta\sigma_{Ex}$ is the error associated with σ_{Ex}, and N is the number of experimental points used in the fit. The normalization factor is denoted by R, and σ_{tot} is the calculated total reaction cross section.

The initial parameters in the search routine were based on published systematic studies[33,34] of 15- and 20-MeV triton elastic scattering. Table I presents the sets of parameters which gave the best fit to our data for 15-MeV tritons on ^{86}Sr. The set of parameters designated Type I is the result of the use of initial parameters taken on the basis of the expressions derived by Hafele, Flynn, and Blair[33]:

$$V = (0.057A + 148)\ \text{MeV},$$

$$W = (-0.097A + 29.4)\ \text{MeV},$$

TABLE I. Sets of parameters which give best fit to ^{86}Sr elastic scattering of 15-MeV incident tritons. Parameters shown underlined were kept fixed during search. Coulomb radius r_0^C=1.25 F for all cases. A total of 29 data points were fitted.

Type	V (MeV)	W (MeV)	r_0 (F)	r_0' (F)	a (F)	a' (F)	σ_{tot} (b)	χ^2
IA	153	25.8	1.24	1.45	0.680	0.806	1.80	0.94
IB	152	25.4	1.24	1.44	0.674	0.820	1.81	0.94
IC	140	26.1	1.32	1.38	0.620	0.868	1.81	0.94
ID	143	23.9	1.30	1.41	0.637	0.842	1.81	0.94
IE	153	31.9	1.23	1.41	0.684	0.806	1.81	0.96
IIA	168	24.1	1.16	1.48	0.726	0.794	1.81	0.98
IIB	170	25.3	1.17	1.47	0.713	0.806	1.82	0.99
IIC	155	21.8	1.23	1.46	0.671	0.838	1.82	1.00
IID	170	23.9	1.16	1.49	0.724	0.797	1.81	0.98
IIE	252	32.1	1.16	1.41	0.684	0.806	1.81	0.95

where the Coulomb radius parameter was taken to be 1.25 F. Since previous studies[33] had not revealed any strong influence of variations in the spin-orbit terms, the latter were not included in the search. The surface-peaked imaginary potential (W_D) was assumed to be zero; only volume absorption was considered. This so-called "150-MeV family" conforms with the suggestion[35] that the real part of the potential for a mass-3 particle should be about 3 times that for a single nucleon.

Another family, characterized by a significantly smaller real radius parameter, has been found to fit the 20-MeV triton elastic scattering data for a number of elements.[34] We investigated this family by initiating the search at $V = 170$ MeV and $r_0 = 1.16$ F. The results are included in Table I under the category Type II. From the χ^2 values in Table I and from the plots of elastic scattering cross sections in Fig. 3, it is apparent that the fits of the two families, as represented by IA and IIA, are equally good, and that the elastic scattering analysis alone does not permit a unique choice of parameters.

The calculated cross sections for the triton elastic scattering were used to determine the target thickness and thus the absolute calibrations for the (t,p) reaction data. At 15 MeV the elastic scattering for angles less than 20° is dominated by Rutherford scattering, and hence is relatively insensitive to the choice of optical-model parameters. Accordingly, the forward-angle data were fitted to achieve the best χ^2 value using the parameters of Set IA, with variation only in the normalization factor R. This factor was then used to renormalize cross sections for the entire angular distributions of tritons and protons. Uncertainty in the cross-section calibration was estimated to be 10%, which constitutes a minimum uncertainty in the reported (t,p) cross sections.

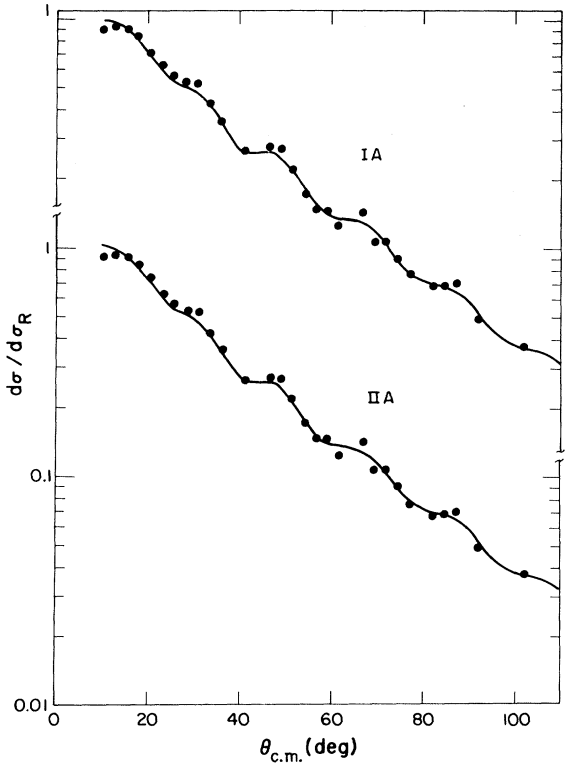

FIG. 3. Elastic scattering of 15.0-MeV tritons from ^{86}Sr. The labels IA and IIA refer to sets of optical-model parameters in Table I.

B. ^{88}Sr Levels

Proton spectra from the ^{86}Sr$(t,p)^{88}$Sr reaction were measured at 2.5° intervals from 12.5 to 90° with the counter-telescope system and at 20, 30, 35, and 40° with the Elbek magnetic spectrograph. Representative spectra are plotted in Figs. 4 and 5.

The ^{88}Sr levels observed in this study are listed in Table II. The level numbers enclosed in parentheses indicate very weak peaks, for which the variation of energy with angle was not sufficiently unambiguous to permit definite assignment to ^{88}Sr. For the 0^+ states, the largest cross sections were observed at the smallest angle studied; since, however, at this angle the angular distributions were changing rapidly and the counting statistics were poor, the cross sections listed are those for the second maximum near 38°. For weak states which have large uncertainties at the angle of peak cross section, the theoretical curve fitted to neighboring points was chosen to represent the cross section; for unresolved doublets and for other levels with insufficient data, the approximate cross sections at 30° are given. Spin-parity assignments are listed in Column 5. For an even-even target nucleus such as ^{86}Sr, the spin-parity values of the ^{88}Sr product states are uniquely determined by the angular momentum transfer in the (t,p) reaction; since the neutron pair in the triton is predominantly in a relative S state, the (t,p) reaction gives $J = L$ and $\pi = (-1)^L$.

Because of the high level density above 5.5 MeV, complete angular distributions could not be obtained for the levels above No. 20. However, sufficient data were obtained to permit provisional assignments for Nos. 25–31, 33–35, 37, and 42. For these and other levels for which firm assignments could not be made the J^π values are enclosed in parentheses.

C. Distorted-Wave Analysis

1. *Angular Momentum Assignments*

Calculations based on the distorted-wave Born approximation (DWBA) were carried out with a

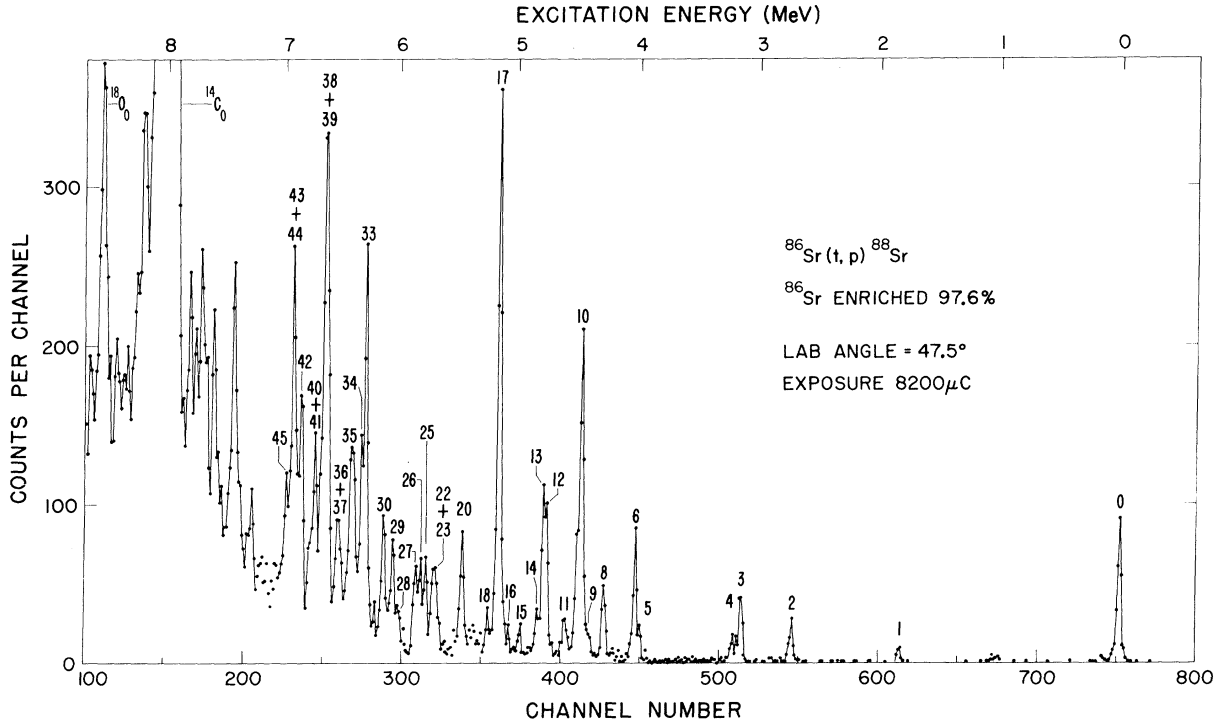

FIG. 4. Proton spectrum at lab angle of 47.5° as measured with the semiconductor telescope arrangement. The numbered peaks are listed in Table II.

zero-range two-nucleon stripping code (TWOPAR) prepared by Bayman and Kallio.[36] Our principal use of the code was to establish the angular momentum transfer and to determine the relative cross sections for various configurations of the transferred neutrons.

The neutrons were assumed to be bound in a Woods-Saxon well with parameters $r_0 = 1.25$ F, r_0(Coulomb) = 1.25 F, and spin-orbit strength $\lambda = 25$; the triton rms radius was assumed to be 1.7 F. The neutron binding energy for each of the transferred neutrons was taken to be one half of the two-neutron binding energy. Spin-orbit coupling was not included in the code. The radial integrations were not conducted with a finite lower cutoff; they were started at the nuclear center.

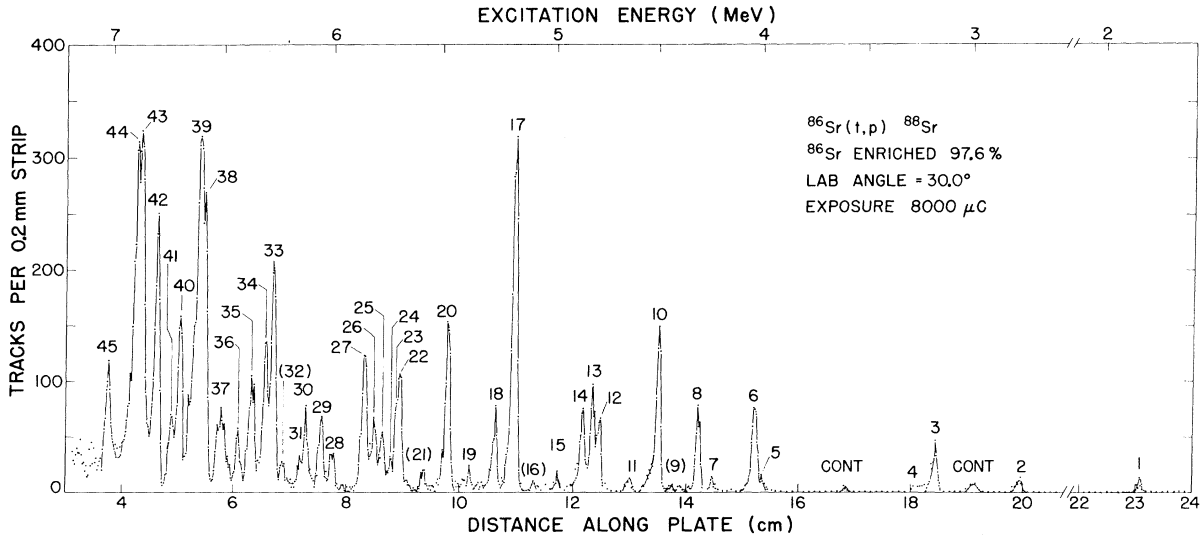

FIG. 5. Proton spectrum at lab angle of 30.0° as measured with the magnetic spectrograph. The numbered peaks are listed in Table II.

TABLE II. Summary of states populated by ^{86}Sr$(t,p)^{88}$Sr with 15-MeV tritons.

Level No.[a]	Energy (keV)	Peak cross section (μb/sr)[b]	c.m. angle at peak cross section[c] (deg)	J^π
0	0	114		0^+
1	1836	18.4		2^+
2	2734	20.7		3^-
3	3151± 3	35.1		0^+
4	3220±10	13.7		2^+
5	3990± 5	10.5	20	$4^+,3^-$
6	4033± 3	100		2^+
7	4232±10	6.0		4^+
8	4298± 3	39.6		4^+
9	4416±10	17.8	20	$[2^+,6^+]$[d]
10	4484± 5	168		0^+
11	4619± 5	45		2^+
12	4763± 3	98		2^+
13	4794± 4	74	43	0^+
14	4838± 4	68	25	(3^-)
15	4983± 3	45		2^+
(16)	5076±10	12.9	20	(1^-)
17	5165± 4	564		2^+
18	5259± 5	49	22	(3^-)
19	5376±10	16.2		4^+
20	5470± 3	85		4^+
(21)	5583±10	~10	30	
22	5685±10	~79	30	
23	5699±10			
24	5724±10	~ 3	30	
25	5766±10	38	40	(0^+)
26	5806±10	65	22	$(3^-,2^+)$
27	5855±10	65	22	(3^-)
28	6005± 5	39	18	(2^+)
29	6048± 3	97	18	(2^+)
30	6123± 3	59	20	(3^-)
31	6149± 6	69	13	(1^-)
(32)	6212±15	~10	30	
33	6270± 4	259	20	(2^+)
34	6307± 3	156	20	(2^+)
35	6362±10	115	20	$(4^+,3^-)$
36	6428± 4	39	20	
37	6512±10	126	18	(2^+)
38	6582±10	~320	30	
39	6605± 3			
40	6691± 3	~100	30	
41	6735±10	~14	30	
42	6804± 4	129	30	(4^+)
43	6874±10	~350	30	
44	6892±10			
(45)	7017±10	~70	30	

[a] Parentheses enclosing a level number indicate an uncertainty in assignment as a level in ^{88}Sr.

[b] Cross sections listed are experimental; in those cases where the data exhibit poor statistics the DWBA results are reported as average values. For unresolvable doublets and for levels with insufficient data, the approximate cross section at 30° is given.

[c] The angle at which the maximum cross section is reported is taken to be 38° for $L=0$, 18° for $L=2$, 22° for $L=3$, and 30° for $L=4$. For distributions where L is in doubt, the experimental results are reported.

[d] Unresolved doublet.

TABLE III. Optical potentials in the ground-state distorted-wave analysis. Each proton set contained also a spin-orbit term [V_{so} (P1) = 8.5 MeV, V_{so} (P2) = 6.4 MeV, V_{so} (P3) = 5.5 MeV, V_{so} (P4) = 6.0 MeV] which was not introduced in the two-nucleon stripping calculations.

Type	V (MeV)	r_0 (F)	a (F)	W_v (MeV)	W_s (MeV)	r_0' (F)	a' (F)	Ref.
Protons								
P1	47.0	1.25	0.650	0	13.4	1.25	0.470	32
P2	55.0	1.12	0.750	3.0	6.7	1.33	0.580	37
P3	57.1	1.14	0.710	0	9.4	1.25	0.470	8
P4	56.1	1.15	0.650	0	8.5	1.25	0.780	8
Tritons								
T1	153	1.24	0.684	25.8	0	1.45	0.806	present work
T2	168	1.16	0.730	24.1	0	1.45	0.790	present work

Since no "best" set of proton and triton optical-model parameters had been worked out for our experimental conditions, some exploratory calculations were carried out. These calculations involved several combinations of previously published proton parameters with our triton parameters from Table I. Four sets of proton parameters (shown in Table III) were used: (1) a set of average parameters taken from Perey's analysis of 19- and 22-MeV proton scattering[32]; (2) a set from Satchler's analysis of 30-MeV proton scattering[37]; (3) and (4), two sets from 19-MeV proton scattering on ^{88}Sr, by Stautberg, Kraushaar, and Ridley.[8] All four contained spin-orbit terms, but these were not used, since the two-particle stripping code had no provision for them. Of the possible sets of triton parameters from Table II, Sets IA and IIA were chosen as being representative.

The various combinations of optical-model parameters were tested by fitting the calculated $L = 0$ angular distributions to the distribution for the (t,p) reaction to the ^{88}Sr ground state. The proton parameters derived directly from elastic scattering on ^{88}Sr (Sets P3 and P4 in Table III) were found to yield considerably better fits than those derived from "averages" (Sets P1 and P2). Fits from combinations of the two best proton sets with the two representative triton sets are shown in Fig. 6. The higher-L transfers were less sensitive to choice of parameters. From Fig. 6 it is evident that the triton parameter set T2 gives a better fit than T1. The slight mismatch in positions of calculated and experimental minima is not considered serious; it could be corrected by a 1.0-MeV increase in the proton real well depth.

The sensitivity of the $L = 0$ distribution, as shown above, could be utilized to reduce the ambiguity in the choice of triton optical potentials. The preference for a smaller triton radius parameter (r_0 = 1.16 F) indicated by our data agrees with the conclusions drawn in studies of (t,p) reactions on Zr isotopes[38] and with an analysis of the ^{90}Zr(p,t) reaction.[39] It should be pointed out, however, that the fitting of (t,p) angular distributions does not uniquely determine the triton parameters; the determination depends on the set of proton parameters used. Thus, Barz *et al.*,[40] using published angular-distribution data for (t,p) reactions on a variety of targets at E_t = 12 MeV, derived a mass-

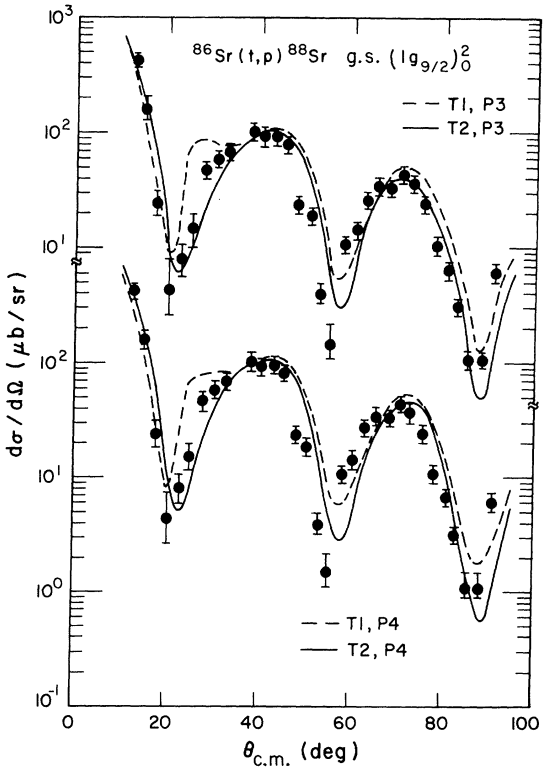

FIG. 6. Calculated angular distributions for the (t,p) transition to the 0^+ ground state of ^{88}Sr. The curves correspond to combinations of proton and triton parameters contained in Table III.

independent set of triton parameters with $V = 155$ MeV and $r_0 = 1.24$ F, based on Perey's average proton parameters.[32]

Our DWBA calculations for $L = 0$ transfer to the ^{88}Sr ground state were carried out for stripping of a $(1g_{9/2})^2_0$ neutron pair. Calculations for stripping into $(2p_{1/2})^2_0$ and $(2p_{3/2})^2_0$ gave different cross sections but qualitatively similar shapes. However, the first minima for the angular distributions based on these configurations were shallower than those for $(1g_{9/2})^2_0$.

We performed the DWBA calculations for all the excited states of ^{88}Sr with the optical-potential sets T2 and P3. For calculation of the $L = 0$, 2, and 4 distributions, the neutrons were assumed to have been stripped into the $(2d_{5/2})^2$ configurations. The $L = 1$, 3, and 5 distributions were obtained with the configurations $(2p_{1/2})(3s_{1/2})$, $(2p_{1/2})(2d_{5/2})$, and $(2p_{3/2})(1g_{7/2})$, respectively. For angular momentum transfers other than zero, the shapes of the angular distributions appeared to be independent of neutron configuration.

Results for the excited 0^+ states are shown in Fig. 7. As may be seen, the fits for the 3.151- and 4.484-MeV levels are satisfactory, although the second minimum in the experimental distribution for the latter is definitely shallower than predicted. The fit for the 4.794-MeV distribution is noticeably poorer; were it not for the data point at 20°, a definite $L = 0$ assignment could not be made. Unfortunately, this level is the center member of a closely spaced triplet, so that intensity measurements were difficult, particularly near the minima in the distribution. It is evident that for all three distri-

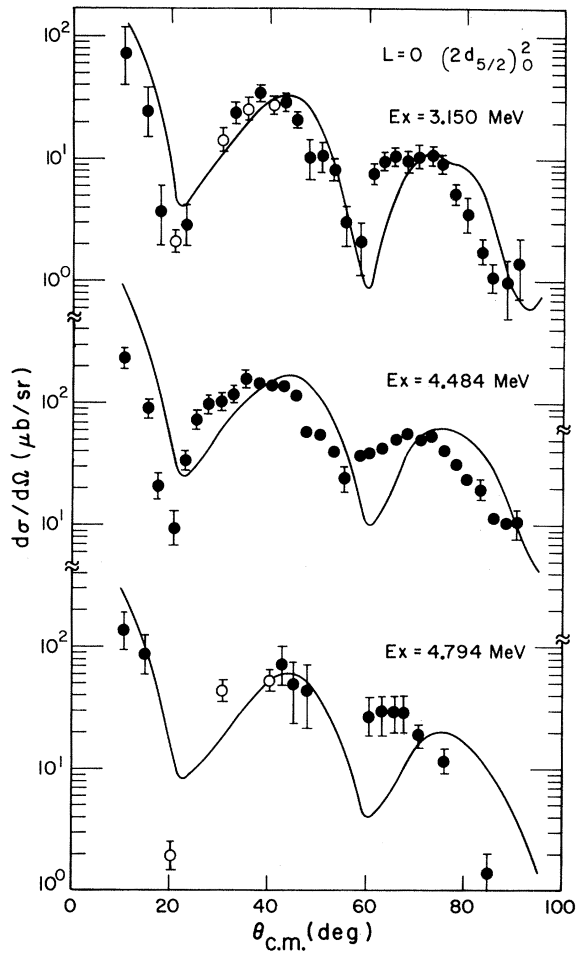

FIG. 7. $L = 0$ transitions for ^{86}Sr$(t,p)^{88}$Sr reaction. Open circles designate data points taken from spectrograph results.

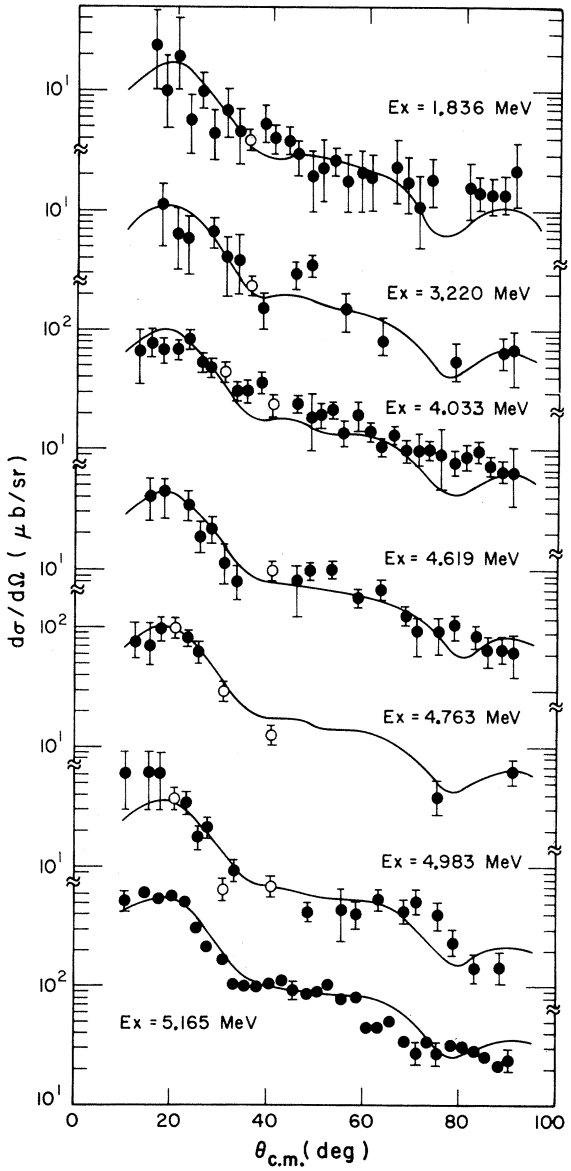

FIG. 8. $L = 2$ transitions for the ^{86}Sr$(t,p)^{88}$Sr reaction.

butions shown, the theoretical diffraction pattern is shifted to higher angles than the corresponding experimental points. There are several structural parameters that could be responsible for this mismatch, exclusive of Q effects, but the patterns were sufficiently distinct to permit L assignments.

Figure 8 shows the results for the $L=2$ distributions. In general, the fits are reasonably good, even for the weakly populated levels. For the strong level at 4.033 MeV, however, the fit is surprisingly poor. Although the peak corresponding to this level forms a doublet with another for the level at 3.990 MeV (Fig. 11), the latter is too weak to constitute a sufficiently serious perturbation. It is possible that there is a third unresolved peak with $L \neq 2$ whose contribution may be responsible for the deviation from the theoretical distribution. We were unable to detect such a peak in the spectrograph results, which implies that it would have to lie within ~10 keV of the 4.033-MeV peak. No other measurements of ^{88}Sr levels have been interpreted as showing evidence of another level in this region.

The results for $L=4$ transfers are shown in Fig. 9. The theoretical fits for the strongly populated states at 4.298 and 5.470 MeV are seen to be very good. Figures 10 and 11 contain distributions for which more than one L assignment is possible. Only the $L=1$ theoretical distribution is shown for the 5.076-MeV level, but the fit of the data does not warrant a firm assignment. The level at 2.734

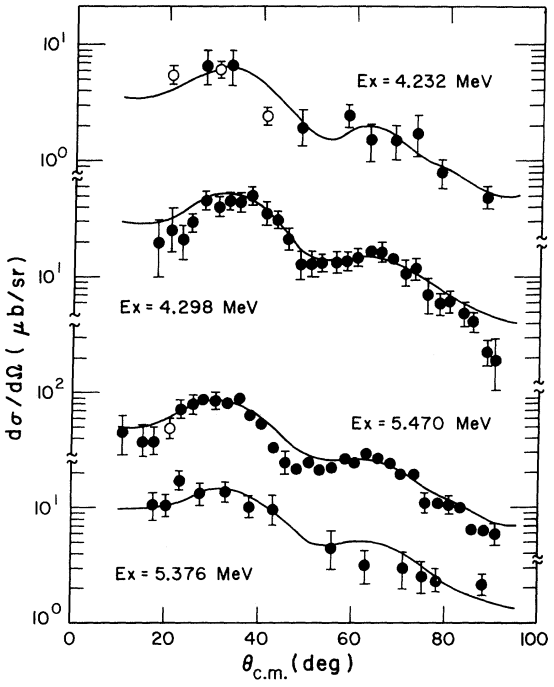

FIG. 9. $L=4$ transitions for the ^{86}Sr$(t,p)^{88}$Sr reaction.

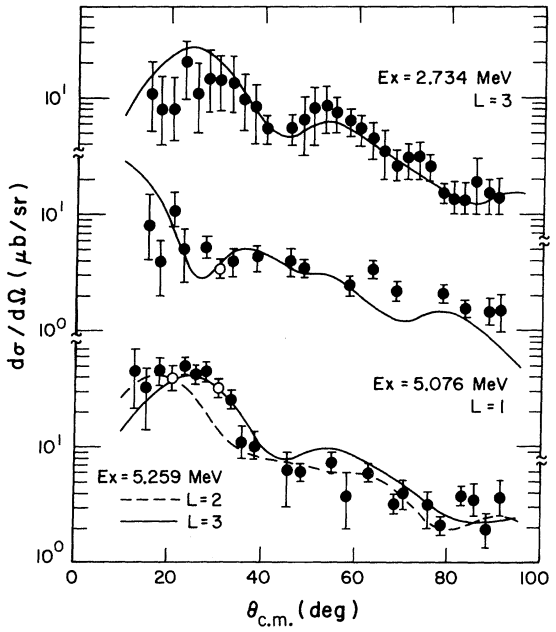

FIG. 10. Various transitions for ^{86}Sr$(t,p)^{88}$Sr reactions to different L values.

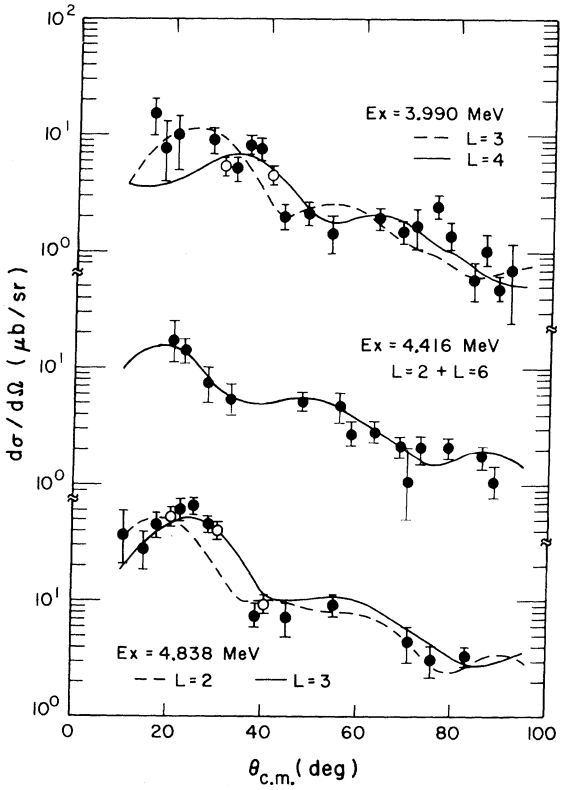

FIG. 11. Various transitions for ^{86}Sr$(t,p)^{88}$Sr reactions to different L values.

MeV is the only firmly established $J^{\pi} = 3^-$ level known in ^{88}Sr; the apparent deviation in the fit at angles below 30° is puzzling.

Above 5.5-MeV excitation energy the levels were so closely spaced that the counter-system resolution in most cases did not permit reliable intensity measurements. Those angular distributions which contained enough data for L assignments are plotted in Figs. 12 and 13. As may be seen, a number of the experimental angular distributions allow relatively unambiguous L assignments in spite of large gaps in the data points.

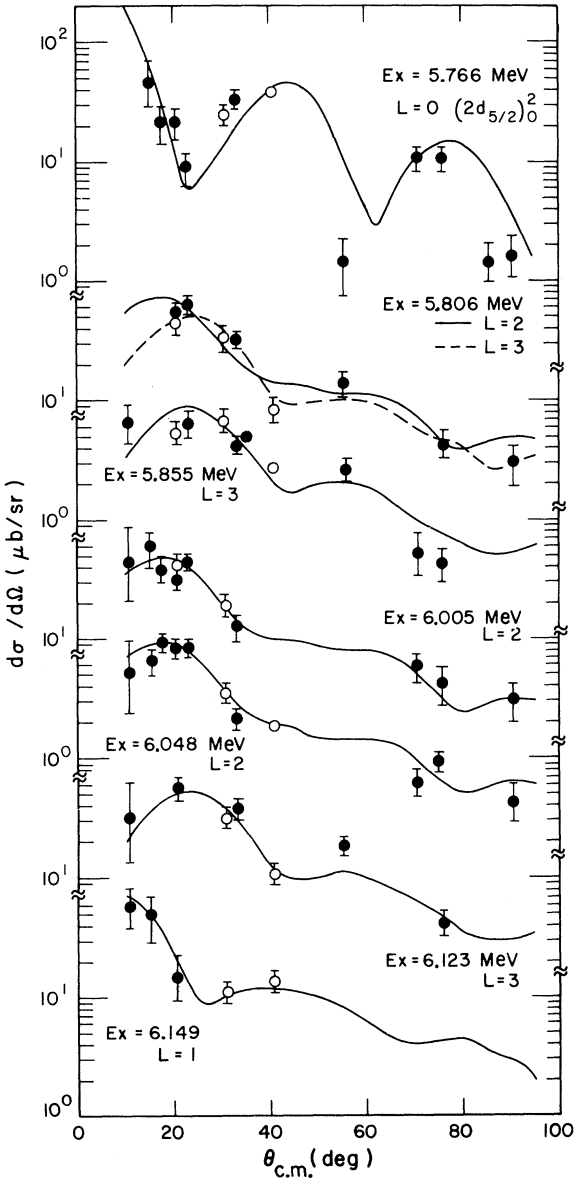

FIG. 12. ^{86}Sr$(t,p)^{88}$Sr transitions to levels above 5.5 MeV. The L assignments are considered tentative because of the relatively few data points for the distributions.

2. $L = 0$ Transitions

Five 0^+ states were observed in ^{88}Sr. Table IV lists their energies and relative cross sections, together with the ^{88}Sr$(t,p)^{90}$Sr ground-state relative cross section. The latter was obtained from a separate bombardment ($\theta_{lab} = 40°$) of a target prepared with ^{86}Sr and ^{88}Sr in a 1:1 ratio. Also shown in the table are relative theoretical cross sections for population of various configurations in ^{88}Sr and ^{90}Sr, calculated with the DWBA two-nucleon transfer code TWOPAR.[36]

The mixed configuration chosen for the theoretical two-neutron transfer cross section used as the

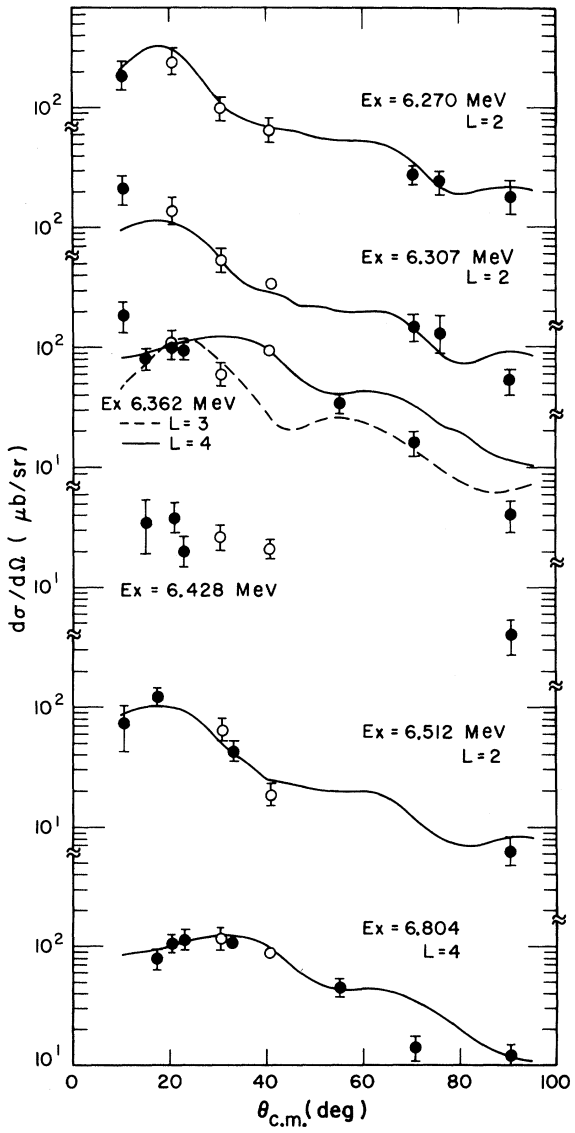

FIG. 13. ^{86}Sr$(t,p)^{88}$Sr transitions to levels above 5.5 MeV. The L assignments are considered tentative because of the relatively few data points for the distributions.

TABLE IV. Comparison of relative experimental peak cross sections with relative calculated peak cross sections of pure and mixed $(nlj)^2$ transfers for $^{86}Sr(t,p)^{88}Sr$ and $^{88}Sr(t,p)^{90}Sr$ $L=0$ transitions at $E_t = 15.0$ MeV.

Excitation energy (MeV)	Experimental $d\sigma/d\Omega$ (relative, at 38°)	Theoretical $d\sigma/d\Omega$ (relative, at 40°) A $(2p_{3/2})^2_0$	B $(2p_{1/2})^2_0$	C $(1g_{9/2})^2_0$	D $(2d_{5/2})^2_0$	E $(3s_{1/2})^2_0$	F $(2d_{3/2})^2_0$	$\begin{pmatrix}0.87C-0.40B\\-0.28A\end{pmatrix}$	$\begin{pmatrix}0.87D\\+0.50E\end{pmatrix}$
$^{86}Sr(t,p)^{88}Sr$									
0	1.00	1.43	0.55	0.19				1.00	
3.151	0.32	1.71	0.68	0.19	2.30	2.36	0.87		
4.484	1.49				2.41	2.55	0.95		4.60
4.794	0.65				2.45	2.60	0.98		
5.766	0.35				2.54	2.76	1.03		
$^{88}Sr(t,p)^{90}Sr$									
0	3.43				2.52				4.83

reference basis for the others was based on recent work on the $^{87}Sr(d,t)^{86}Sr$ reaction,[41] which indicated that 76% of the neutron part of the ^{86}Sr ground-state wave function is contained in the $(1g_{9/2})^{-2}$ term. The remaining 24% we assigned to $(2p_{1/2})^{-2}$ and $(2p_{3/2})^{-2}$ in the intensity ratio 2:1. As may be seen from the results for the pure configurations, the cross section is sensitive to the amount of $(2p_{3/2})^{-2}$. The effect of configuration mixing is shown also for the 4.484-MeV state of ^{88}Sr and the ground state of ^{90}Sr, where a trial mixture of 75% $(2d_{5/2})^2$ and 25% $(3s_{1/2})^2$ was transferred.

From a comparison of the relative experimental with the relative calculated cross sections, it appears that the ratio of experimental ^{88}Sr and ^{90}Sr ground-state cross sections could be satisfied by reasonable configuration mixtures for the transferred neutrons. The experimental cross sections for the ^{88}Sr 0^+ excited states are smaller than expected, however, particularly from the viewpoint of the pairing-vibration model. According to this model, the Q value for the (t,p) reaction leading to the ^{88}Sr pairing-vibration state should approximately equal the Q value for the $^{88}Sr(t,p)^{90}Sr$ ground-state reaction, and the cross sections should be equal.[42] In this harmonic approximation based on the assumptions that the protons are spectators in the neutron transfer process and that the neutron particles and holes do not interact, the ^{88}Sr pairing vibration should occur at 5.36 MeV. However, the population of the three 0^+ states at 4.484, 4.794, and 5.766 MeV totals only 2.5 on the scale on which the $^{88}Sr(t,p)^{90}Sr$ cross section is 3.4, and their energies and relative populations suggest that the pairing-vibration strength may be fragmented. Since the amplitude of the (t,p) reaction leading to a given level is a coherent sum over the contributions of the individual terms, the total cross section is sensitive to mixing.

A similar experimental situation exists for the $^{92}Zr(p,t)$ reaction leading to 0^+ states in ^{90}Zr (data in Fig. 14 taken from Ball, Auble, and Roos[43]), where the pairing vibration should lie at 5.31 MeV. The centroids of these states lie at 4.90 MeV in ^{90}Zr and 4.75 MeV in ^{88}Sr, and the summed 0^+ cross sections are 75 and 72% of the $^{90}Zr(p,t)^{88}Zr$ and $^{88}Sr(t,p)^{90}Sr$ ground-state cross sections, respectively. Thus, it appears likely that similar mechanisms may be responsible for the missing pairing-vibration strength in both closed-shell nuclei. Sørensen[44] has suggested that the fragmentation in ^{90}Zr might be due to interaction with two-phonon quadrupole and octupole states, which should be located in the region of 4–5 MeV excitation for both ^{88}Sr and ^{90}Sr.

IV. DISCUSSION

Table V presents a comparison of our $^{86}Sr(t,p)$-^{88}Sr results with other high-resolution data on the ^{88}Sr levels. The results of the inelastic scattering experiments have been discussed previously,[17] and are not included here. For comparisons of this kind, a critical point is the identification of the same level in different experiments. The energy agreements as shown in Table V are, in general, satisfactory; consequently, the data among the five modes of population can in most cases be compared with some confidence. For the levels at 4.033, 4.298, 5.470, 6.005, and probably also 4.416 MeV, our (t,p) results remove the J^π ambiguity from the (d,p) results.[15] For the levels at 2.734, 3.220, 5.165, and 6.048 MeV, the (t,p) results permit assignment of J^π values, while the (d,p) studies indicate nonstripping distributions due presumably to secondary processes. However, there are several levels for which our J^π assignments appear to conflict with the (d,p) results.

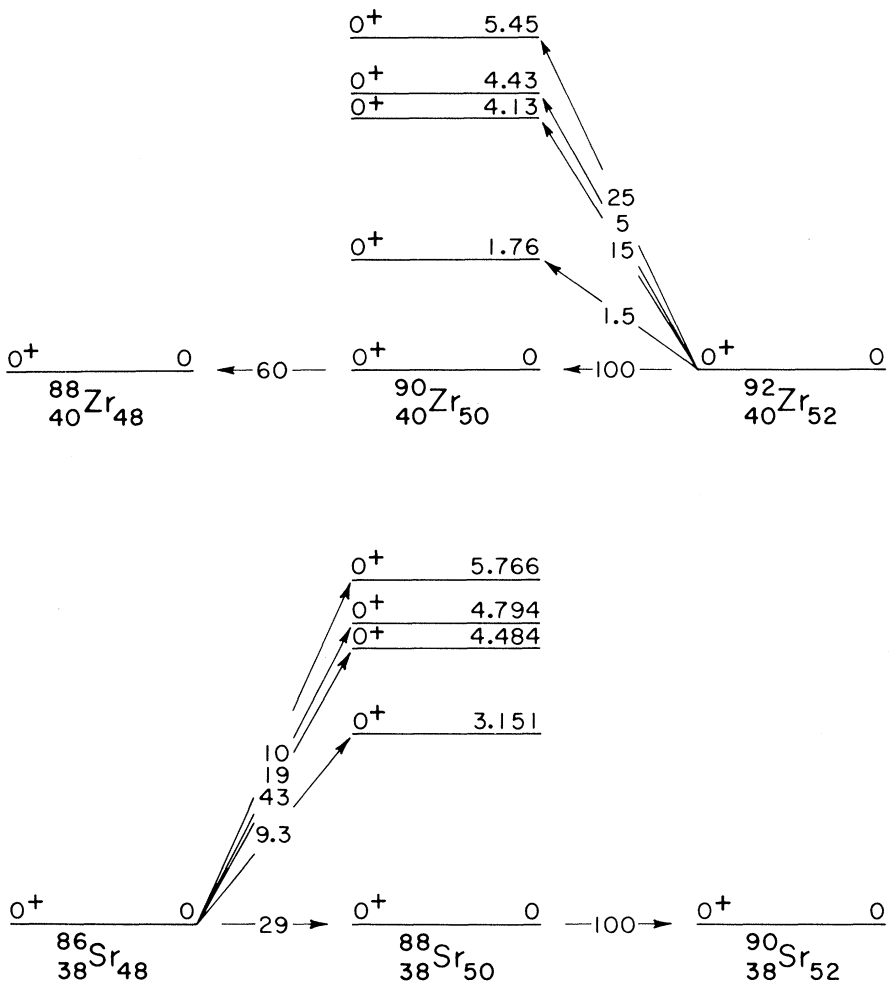

FIG. 14. Comparison of the $L=0$ transitions for the ^{92}Zr$(p,t)^{90}$Zr reaction and the ^{86}Sr$(t,p)^{88}$Sr reaction. The cross sections for the ground-state transitions between the 50-neutron and 52-neutron nuclei have been normalized to 100.

Both the (t,p) and (d,p) measurements show a level at 6.149 MeV, but the former lead to a tentative assignment of $J^\pi = 1^-$ (see Fig. 12), whereas the latter indicate $l_n = 2$ (i.e., $J^\pi = 2^+ - 7^+$). Although the (t,p) distribution for this transition contains only five points, the fit is good, and likewise the (d,p) data points for this level show a good fit to $l_n = 2$. There is a similar conflict for the level at 6.512 MeV; the (d,p) results suggest a 4, 5^+ assignment, but the (t,p) assignment is tentatively 2^+.

We can use the results of the study[17] of the β decay of ^{88}Rb to resolve the J^π ambiguity for the 3.990-MeV level. If $J^\pi = 3^-$, the level should be populated by an allowed β transition from ^{88}Rb. Since there was no evidence of β population of such a level, we conclude that the $J^\pi = 4^+$ alternative is the correct one; β decay to a 4^+ state would involve a first-forbidden unique transition, with an expected intensity ~10^3 lower than for an allowed transition, a result consistent with the reported decay scheme.

The J^π ambiguity of level No. 14 at 4.838 MeV cannot be eliminated in this manner. Although a 3^- level at 4.845 MeV has been observed in ^{88}Rb decay and in the ^{87}Sr(n,γ) reaction, the difference in energies appears to lie outside the assigned error limits and thus does not permit identification of the levels as one and the same.

The angular distribution for the apparent level at 4.416 MeV (Fig. 11) could not be fitted by the theoretical distribution for any single L value. It could be represented well, however, as the sum of distributions of an unresolved $(L=2)$-$(L=6)$ doublet. From best fits of the theoretical angular distributions to the data, the magnitudes of $d\sigma/d\Omega$ at 18° for the two components were 14.1 and 0.83 μb/sr. The $J^\pi = 2^+$ member of the doublet may be identified with the 4.414-MeV level observed in ^{88}Rb β decay

TABLE V. ^{88}Sr levels populated by various reactions.

No.	This work Energy (MeV)	J^π	^{88}Rb decay[a] Energy (MeV)	J^π	(t,α)[b], $(d,^3\mathrm{He})$[c] Energy (MeV)	J^π	(d,p)[d] Energy (MeV)	l_n	(n,γ)[e] Energy (MeV)	J^π
0	0	0^+	0	0^+	0	0^+	0	4	0	0^+
1	1.836[f]	2^+	1.836	2^+	1.836	2^+	1.839	2	1.836	2^+
2	2.734[f]	3^-	2.734	3^-			2.738	ns[g]	2.734	3^-
3	3.151	0^+			3.156					
4	3.220	2^+	3.220	2^+	3.221	(2^+)	3.208	ns	3.220	2^+
			3.488	(1^+)	3.489	(1^+)			3.487	1^+
									3.523	$(+)$[h]
							(3.590)	ns	3.585	(4^-)[f]
			3.635	(3^+)	3.635	(3^+)			3.635	3^+
									3.691[g]	$(+)$[h]
					3.946				3.953	
5	3.990	$4^+,3^-$			3.985					
6	4.033	2^+			4.029		4.035	2		
					4.154					
									4.170	$(4,5^-)$[f]
7	4.232	4^+							4.227	$(4,5^-)$[f]
									4.269	
					4.287					
8	4.298	4^+					4.294	2	4.301	
9	4.416	$[2^+,6^+]$[i]	4.414	$(3,2^+)$			4.408	2	4.414	
					4.428					
							4.450	2	4.452	$(4,5^-)$[f]
							4.464	ns		
10	4.484	0^+								
			4.513	$(2,3^-)$			4.514	2	4.514	(2^-)[h]
							4.551			
					4.607					
11	4.619	2^+								
							4.636	2		
			4.745	(2^+)	4.751		(4.748)	(2)	4.743	
12	4.763									
13	4.794	0^+					4.789			
14	4.848	(3^-)	4.845	(3^-)					4.846	3^-
			4.854	(2^-)						
					4.881		4.876	0		
					4.909		4.920	ns		
15	4.983	2^+			4.974					
									5.011	$(3,4)$[f]
16	5.076	(1^-)			5.075				5.077	
							5.101	2		
							5.133			
17	5.165	2^+					5.157	ns		
							5.199	ns		
18	5.259	(3^-)							5.263	
									5.321	(3)[f]
19	5.376	4^+								
							5.418	0		
					5.426				5.426	(3)[f]
20	5.470	4^+					5.463	0		
							5.506	0		
									5.518	
									5.537	
21	5.583									
							5.665	(1)	5.662	
									5.690	
22	5.685									
23	5.699									

TABLE V *(Continued)*

No.	This work Energy (MeV)	J^π	^{88}Rb decay[a] Energy (MeV)	J^π	(t,α)[b], $(d,^3\mathrm{He})$[c] Energy (MeV)	J^π	(d,p)[d] Energy (MeV)	l_n	(n,γ)[e] Energy (MeV)	J^π
24	5.724						5.719	0		
									5.751	
25	5.766	(0^+)					(5.775)	(0)		
26	5.806	$(3^-,2^+)$							5.811	
							5.830		5.836	
27	5.855	(3^-)								
							5.876	ns	5.952	
28	6.005	(2^+)					6.008	2		
29	6.048	(2^+)					6.043	ns		
30	6.123	(3^-)							6.124	
31	6.149	(1^-)					6.149	2		
32	6.212						6.214	0		
							6.237	(1)		
									6.258	
33	6.270	(2^+)								
34	6.307	(2^+)					6.306			
							6.340	2		
35	6.362	$(4^+,3^-)$								
							6.376	(2)		
									6.388	
36	6.428						6.420	(2)		
							6.465	2		
37	6.512	(2^+)					6.515	(0)		
							6.564	2		
38	6.582									
							6.612	ns		
							6.629	ns		
40	6.691						6.687	ns		
							(6.719)	ns		
41	6.735						6.740			
							6.752			
42	6.804	(4^+)								
							6.826	2		
43	6.874						6.869			
44	6.892									
							6.931	2		
							6.958	2		
45	7.017									
							7.026	ns		

[a] See Ref. 17.
[b] The level energies listed are taken from the (t,α) results (Ref. 14).
[c] The spin-parity assignments listed are taken from the $(d,^3\mathrm{He})$ results (Ref. 13).
[d] See Ref. 15, levels above 7.026 MeV not included in this list.
[e] See Ref. 26, unless otherwise noted.
[f] See Ref. 23.
[g] Nonstripping angular distributions.
[h] See Ref. 24.
[i] Unresolved doublet.

and in ^{87}Sr(n,γ). The $J^\pi = 6^+$ member appears to be the 4.408-MeV level observed in the ^{87}Sr(d,p) work[15] and will be discussed subsequently in this section.

Hughes[5] has calculated the ^{88}Sr level structure using phenomenological two-body matrix elements. His calculations involved proton states based on two holes in the $(1f_{7/2})$, $(1f_{5/2})$, $(2p_{3/2})$, and $(2p_{1/2})$ orbitals, and neutron 1p-1h states resulting from the coupling of a $(1g_{9/2})$ hole with $(2d_{5/2})$, $(3s_{1/2})$, $(2d_{3/2})$, and $(1g_{7/2})$ particles. Figures 15 shows a comparison of his proton and neutron level calculations with our (t,p) data. We point out that he did not attempt to calculate the positions of any odd-parity levels with either proton or neutron configurations. Our (t,p) levels are plotted such that the lengths of the lines are proportional to $(d\sigma/d\Omega)_{\max}/$

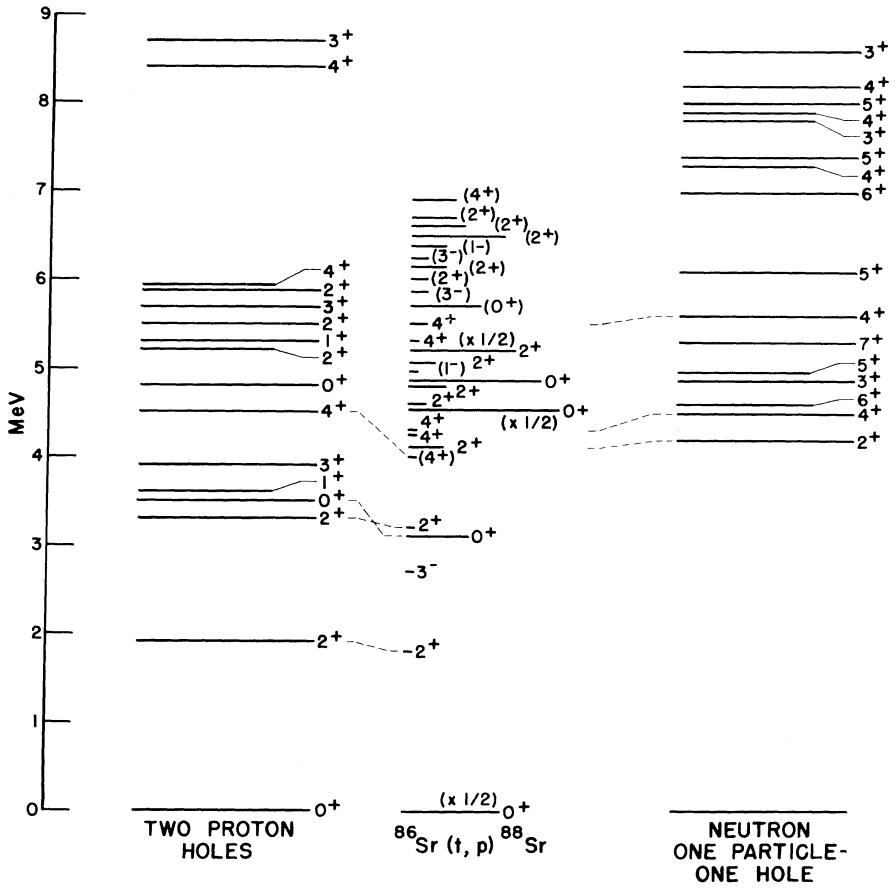

FIG. 15. Comparison of levels from the ^{86}Sr$(t,p)^{88}$Sr reaction with theoretical calculations by Hughes (Ref. 5) based on two proton holes in the $Z=40$ subshell and neutron 1p-1h excitations of the $N=50$ core. The lengths of the lines are proportional to $(d\sigma/d\Omega)_{\max}/(2J+1)$.

$(2J+1)$. We do not show levels for which the J^π value was ambiguous or unknown. The dotted lines indicate that extant experimental evidence has established a correspondence between calculated levels and experimental levels.

All of the levels below 4 MeV are primarily proton excitations. From ^{89}Y$(d,{}^3\mathrm{He})^{88}$Sr studies, Kavaloski *et al.*[13] concluded that the $\pi[(2p_{3/2})^{-1}(2p_{1/2})]_{2^+}$ and $\pi[(1f_{5/2})^{-1}(2p_{1/2})]_{2^+}$ configurations account for 80% of the 2_1^+ state (at 1.836 MeV) and 60% of the 2_2^+ state (at 3.220 MeV). Cosman and Slater[15] concluded that most of the neutron strength of the 2_2^+ state is due to $\nu[(1g_{9/2})^{-1}(2d_{5/2})]_{2^+}$ and that no 1p-1h neutron couplings participate in the 2_2^+ state. Unlike the (d,p) reaction, the (t,p) reaction populates the 2_1^+ and 2_2^+ states almost equally. With the two-neutron stripping code,[36] the cross section for a $\nu[(1g_{9/2})^{-1}(2d_{5/2})]_{2^+}$ configuration comes out to be approximately equal to that for a $\nu(2d_{5/2})^2_{2^+}$ configuration for both the 2_1^+ and 2_2^+ states. Thus, it appears that the (t,p) reaction populates the 2_1^+ state mainly via the $\nu[(1g_{9/2})^{-1}(2d_{5/2})]_{2^+}$ component which is fragmented from the 4.033-MeV 2^+ state, and the 2_2^+ state is populated mainly via the $\nu(2d_{5/2})_{2^+}{}^2$ component which is fragmented from a higher 2^+ state.

Both the (d,p) and (t,p) reactions populate the 3^- level at 2.734 MeV weakly, thus indicating only weak neutron admixtures, as expected. The strength of the level is almost entirely contributed by proton 1p-1h excitations. Shastry and Saha[3] calculate that 14 1p-1h proton configurations make up this level, with the largest term being $\pi[(2p_{2/3})^{-1}(1g_{9/2})]_{3^-}$. The (t,p) reaction populates the $\nu[(2p_{1/2})^{-1}(2d_{5/2})]_{3^-}$ and $\nu[(2p_{3/2})^{-1}(2d_{5/2})]_{3^-}$ terms in the neutron components of the wave function. The level at 3.990 MeV, which we assign as most likely $J^\pi=4^+$, is also weakly seen in the (t,α) reaction.[14] This should be the lowest of the proton 4^+ states predicted by Hughes[5]; he calculates an excitation energy of 4.55 MeV and a wave function in which the dominant term (90%) is $\pi[(2p_{3/2})^{-1}(1f_{5/2})^{-1}]$. Since the (t,α) reaction can populate this 4^+ state only by way of its small $(2p_{1/2})^{-1}(1f_{7/2})^{-1}$ term, the

cross section is expected to be small.

The first excited 0^+ state occurs at 3.151 MeV, and should represent mainly proton excitations; Hughes's calculations[5] predict a proton 0^+ state at 3.55 MeV. In the wave functions calculated for this and for the ground state, the amplitudes of the $(2p_{1/2})^{-2}$ term are −0.475 and +0.833, respectively, from which it may be estimated that proton pickup from ^{89}Y should populate the two states in the intensity ratio 0.32, neglecting energy dependence. The observed intensity ratio for the ^{89}Y$(t,\alpha)^{88}$Sr reaction at $E_t = 20$ MeV[14] is 0.22 ± 0.04, in reasonable agreement with the prediction. The ^{86}Sr(t,p)-^{88}Sr reaction populates the 3.151-MeV state also, with an intensity ratio $I(3.151)/I(\text{g.s.}) = 0.32$ (see Table II), but this datum does not permit a quantitative interpretation. Population of the 3.151-MeV state can occur by way of differences in proton wave function between the ^{86}Sr target state and the ^{88}Sr product states, or by way of neutron excitation from fragmentation from higher neutron 0^+ states. The 3.151-MeV level was not observed in the (d,p) work[15]; from the cross-section limits reported for the transitions on either side of it, its population would be less than about 0.3 of that of the ground state.

Cosman and Slater[15] point out that the cluster of eight $l_n = 2$ levels which they observe at 4.035, 4.294, 4.408, 4.450, 4.514, 4.636, 4.748, and 5.101 MeV from the (d,p) reaction should contain large components of the $\nu[(1g_{9/2})^{-1}(2d_{5/2})^1]$ sextuplet. The first two are observed in the (t,p) reaction at 4.033 and 4.298 MeV and are identifiable as $J^\pi = 2^+$ and 4^+, and the third may be identified with the $J^\pi = 6^+$ member of the double level observed at 4.416 MeV. From best fits of the theoretical angular distributions to the data, the magnitudes of $d\sigma/d\Omega$ at 30° for the (t,p) transitions to these three states are in the ratio 1.00:0.91:0.033. The corresponding theoretical ratios for the $L = 2$, 4, and 6 members of the $\nu[(1g_{9/2})^{-1}(2d_{5/2})^1]$ sextuplet, based on the two-neutron stripping code,[36] are 1.00:0.94:0.33. The relative positions and spacings of these levels are in good agreement with the predictions of Hughes for this configuration. None of the remaining members of the cluster were observed in the (t,p) experiments, suggesting that they represent the non-natural-parity members of the multiplet. A complication in any attempt to derive configuration information from these data is that the observed states contain proton excitations also. It has been observed in the ^{89}Y(t,α) work,[14] for example, that the 4.033-MeV state is populated with 0.85 of the strength of the transition to the 1.836-MeV state.

Of the members of the $l_n = 0$ cluster observed in the (d,p) work and interpreted as containing most of the strength of the $\nu[(1g_{9/2})^{-1}(3s_{1/2})^1]$ doublet, one, a 4^+ state at 5.470 MeV, is observed also in the (t,p) experiments; it is, in fact, the strongest $L = 4$ transition that is definitely identified. One other member of the cluster, at 5.724 MeV, was seen also in the (t,p) spectra but was too weak to permit a determination of the angular momentum transfer.

In the excitation region spanned in the present work, the 2^+ state at 5.165 MeV is the most strongly populated, and its energy suggests that it represents the predominant strength of the $\nu(2d_{5/2})^2_{2^+}$ configuration. In this case, it should represent also a large part of the pairing-vibration 2^+ coupling corresponding to the 0.835-MeV first 2^+ state of ^{90}Sr. This is very likely the same level as reported at 5.157 MeV in the (d,p) experiments; the observation that in the latter it is populated only weakly, and with a nonstripping angular distribution, is consistent with the configuration assignment given above.

ACKNOWLEDGMENTS

We wish to thank Dr. W. A. Sedlacek for developing a technique for preparing ^{86}Sr targets by molecular plating of strontium on thin carbon foils. We also thank I. K. Kressin and L. D. Allen for preparing the evaporated ^{86}Sr targets. We appreciate the considerable work done by the Van de Graaff staff in providing the beams and many of the facilities for our experiments. We thank Dr. T. A. Hughes for sending us his calculations on ^{88}Sr levels, and Professor B. F. Bayman for the use of his DWBA code. We also express our appreciation to Dr. G. A. Cowan for his interest and support.

---

*Work supported by the U. S. Atomic Energy Commission.

†Present address: Washington State University, Pullman, Washington 99163.

[1]Talmi and I. Unna, Nucl. Phys. 19, 225 (1960).

[2]N. Auerbach and I. Talmi, Nucl. Phys. 64, 458 (1965).

[3]S. Shastry and A. K. Saha, Nucl. Phys. A97, 567 (1967).

[4]S. Shastry, Phys. Letters 28B, 85 (1968).

[5]T. A. Hughes, Phys. Rev. 181, 1586 (1969); and private communication.

[6]V. Gillet, B. Giraud, J. Picard, and M. Rho, Phys. Letters 27B, 483 (1968).

[7]R. J. Lombard, Phys. Rev. Letters 21, 102 (1968); Nucl. Phys. A117, 365 (1968).

[8]M. M. Stautberg, J. J. Kraushaar, and B. W. Ridley, Phys. Rev. 157, 977 (1967).
[9]J. Picard, O. Beer, A. El Behay, P. Lopato, Y. Terrien, G. Vallois, and R. Shaeffer, Nucl. Phys. A128, 481 (1969).
[10]E. W. Hamburger, Nucl. Phys. 39, 138 (1962).
[11]J. Alster, D. C. Shreve, and R. J. Peterson, Phys. Rev. 144, 999 (1966).
[12]G. A. Peterson and J. Alster, Phys. Rev. 166, 1136 (1968).
[13]C. D. Kavaloski, J. S. Tilley, D. C. Shreve, and N. Stein, Phys. Rev. 161, 1107 (1967).
[14]D. C. Williams, J. D. Knight, and W. T. Leland, Los Alamos Scientific Laboratory, private communication.
[15]E. R. Cosman and D. C. Slater, Phys. Rev. 172, 1126 (1968).
[16]R. N. Glover and A. McGregor, Phys. Letters 24B, 97 (1967).
[17]R. C. Ragaini and J. D. Knight, Nucl. Phys. A125, 97 (1969).
[18]R. Hess, F. C. Roehmer, F. Gassmann, and T. Ledebur, Nucl. Phys. A137, 157 (1969).
[19]H. Lycklama, N. P. Archer, and T. J. Kennett, Can. J. Phys. 47, 393 (1969).
[20]A. Luukko and P. Holmberg, Comment Phys. Math. 33, No. 12 (1968).
[21]N. K. Aras, E. Eichler, G. Chilosi, G. D. O'Kelley, and N. R. Johnson, Nucl. Sci. Appl. 3, 58 (1967).
[22]See references contained in C. M. Lederer, J. M. Hollander, and I. Perlman, *Table of Isotopes* (John Wiley & Sons, Inc., New York, 1967), 6th ed.
[23]J. L. Irigaray, G. Y. Petit, P. Carlos, B. Maier, R. Samama, and H. Nifenecker, Nucl. Phys. A113, 134 (1968).
[24]H. Schmidt, W. Michaelis, C. Weitkamp, and G. Marcus, Z. Physik 194, 373 (1966).
[25]N. C. Rasmussen, Y. Hukai, T. Inouye, and V. J. Orphan, Massachusetts Institute of Technology Report No. MITNE-85, 1967 (unpublished).
[26]H. Lycklama and T. J. Kennett, Nucl. Phys. A139, 625 (1969).
[27]J. Borggren, B. Elbek, L. Perch Nielsen, Nucl. Instr. Methods 24, 1 (1963).
[28]F. S. Goulding, D. A. Landis, J. Cerny, and R. H. Pehl, Nucl. Instr. Methods 31, 1 (1964).
[29]D. D. Armstrong, J. G. Beery, E. R. Flynn, W. S. Hall, P. W. Keaton, Jr., and M. P. Kellogg, Nucl. Instr. Methods 70, 69 (1969).
[30]J. H. E. Mattauch, W. Thiele, and A. H. Wapstra, Nucl. Phys. 67, 1 (1965).
[31]J. B. Marion, Nucl. Data A4, 301 (1968).
[32]F. G. Perey, Phys. Rev. 131, 745 (1963).
[33]J. C. Hafele, E. R. Flynn, and A. G. Blair, Phys. Rev. 155, 1238 (1967).
[34]E. R. Flynn, D. D. Armstrong, J. G. Beery, and A. G. Blair, Phys. Rev. 182, 1113 (1969).
[35]R. M. Drisko, G. R. Satchler, and R. H. Bassel, Phys. Letters 5, 347 (1963).
[36]B. F. Bayman and A. Kallio, Phys. Rev. 156, 1121 (1967); see also B. F. Bayman and N. M. Hintz, *ibid.*, 172, 1113 (1968).
[37]G. R. Satchler, Nucl. Phys. A92, 273 (1967).
[38]J. G. Beery, Los Alamos Scientific Laboratory Report No. LA-3958, 1968 (unpublished).
[39]J. B. Ball, R. L. Auble, R. M. Drisko, and P. G. Roos, Phys. Rev. 177, 1699 (1969).
[40]H. W. Barz, K. Hehl, C. Riedel, and R. A. Broglia, Nucl. Phys. A122, 625 (1968).
[41]R. W. Bercaw and R. E. Warner, Phys. Rev. C 2, 297 (1970).
[42]A. Bohr, in *International Symposium on Nuclear Structure, Dubna, 1968* (International Atomic Energy Agency, Vienna, Austria, 1969).
[43]J. B. Ball, R. L. Auble, and P. G. Roos, Phys. Letters 29B, 172 (1969).
[44]B. Sørensen, Nucl. Phys. A134, 1 (1969).